[Oga* 4(2): February, 2017]
ISSN 2349-4506
Impact Factor: 2.785

Global Journal of Engineering Science and Research Management

THE EFFECT OF MESOPOROUS SILICA-ALUMINA AND IRON LOADING ON CATALYTIC CRACKING OF BIO-OIL

Takahiro Oga*, Ayano Nakamura, Kenji Murakami

* Department of Engineering in Appied Chemistry, Faculty of Engineering and Resource Science, Akita University, 1－1 Tegata gakuen-machi, Akita city, Akita 010-8502 JAPAN
Department of Engineering in Appied Chemistry, Faculty of Engineering and Resource Science, Akita University, 1－1 Tegata gakuen-machi, Akita city, Akita 010-8502 JAPAN
Department of Engineering in Appied Chemistry, Faculty of Engineering and Resource Science, Akita University, 1－1 Tegata gakuen-machi, Akita city, Akita 010-8502 JAPAN

DOI: 10.5281/zenodo.290232

KEYWORDS: bio-oil, catalytic cracking, iron, mesoporous, deoxygenation.

ABSTRACT

Catalytic cracking of bio-oil derived from woody biomass (Japanese cedar) was carried out at 450°C, ambient pressure under He atmosphere using mesoporous silica-alumina (MSAl), iron loaded mesoporous silica (MS/Fe) and iron loaded mesoporous slica-alumina (MSAl/Fe). The bio-oil before and after cracking were characterized by ultimate analysis, GC/MS and FT-IR measurement. When MSAl catalysts (Al = 1, 5, 10 mol%) were used, H/C and O/C of the reformed bio-oil decreased with increasing the Al content. In contrast, when MS/Fe catalysts (Fe = 1, 5, 10 wt%) were used, H/C and O/C of the reformed bio-oil increased with increasing Fe loading. Moreover, when MSAl/Fe catalysts (Al = 1, 5, 10 mol% and Fe = 10wt%) were used, O/C in the reformed bio-oil decreased with increasing Al content while H/C did not decrease. From the Van Krevelen diagram, it was proved that MSAl/Fe catalysts, which contains both of Al and Fe, promoted decarboxylation reaction as well as dehydration. The results of GC/MS analysis mainly showed that the bio-oils before and after cracking were rich in phenols. Interestingly, the FT-IR spectra of the bio-oil indicated that decomposition of conjugated ketones proceeded in MSAl/Fe catalysts, which is possibly related to the decarboxylation reaction.

INTRODUCTION

Energy resources are essential to modern society, not only for heating and cooking but also for power supply and transportation. Petroleum oil is widely used after it is separated into different fuel components such as gasoline, diesel, and heavy fuel oil. These separated fuels are utilized in various processes depending on their fuel properties. Although demand for petroleum oil exists around the world, it has the disadvantage of localization: 47.3% of the proven reserves are concentrated in the Middle East, per the BP Statistical Review of World Energy in June 2016. For this reason, many studies have been conducted into the transformation of various energy resources into alternative liquid fuels. Biomass-to-liquid conversion and coal and gas to liquid fuel conversions are methods that work.

The technique for producing fuel from biomass resources other than foods (e.g. lignocellulosic biomass like wood) has been widely studied. However, the conversion of lignocellulosic biomass to liquid fuel is impeded by the strong bonding between polysaccharides and lignin [1,2]. Therefore, one of the effective conversion methods is a fast pyrolysis of biomass (temperature: 450-550 °C, heating rate: 10^3-10^4 K s^{-1}, in the absence of air, and at atmospheric pressure) [3]. The fast pyrolysis of biomass is a kind of thermochemical process, where cellulose, hemicellulose and lignin are depolymerized and can be converted to liquid bio-oil. However, the elemental composition of the obtained liquid product is different from that of petroleum oil. The bio-oil is composed of various oxygenated compounds such as carboxylic acids, aldehydes, ketones, phenols and alcohols. As the bio-oil contains many oxygen-containing compounds [4], it has a high oxygen content (35–40 wt%) [5]. This results in certain unfavorable properties [5] such as high acidity (pH 2.5), low heating value (16–19 MJ kg^{-1}), and instability, and it cannot be utilized as fuel as it is. A reforming process is necessary to upgrade the properties of the bio-oil by decomposing oxygenated compounds.

These reforming processes for bio-oil are classified into two methods: hydrodeoxygenation and catalytic cracking [3,6]. In hydrodeoxygenation (temperature: 300–400 °C, hydrogen pressure: 80–300 bar, reaction time: 0.2–4 h) [6], hydrogen gas is added to the bio-oil and binds to oxygen to form water, which is then removed. The oxygen content of the reformed bio-oil decreases to less than 5 wt%, so that the heating value increases to 42–45 MJ kg^{-1}, which is comparable to that of petroleum oil [6]. Although hydrodeoxygenation is a suitable process for obtaining a high yield of high-grade oil with low oxygen content, the operating cost is high due to the requirement for a large hydrotreating reactor and high hydrogen consumption (4–7 wt% to bio-oil) [7]. In contrast, catalytic cracking is conducted under ambient pressure without hydrogen. Accordingly, deoxygenation by catalytic cracking is achieved at lower cost than the hydrodeoxygenation method. Generally, the heating value of reformed bio-oil obtained from catalytic cracking is 21–36 MJ kg^{-1} [6]. Williams and Horne performed catalytic cracking of bio-oil using HZSM-5 at 450–550 °C [8]. The yield of reformed bio-oil was 12 wt% relative to the raw bio-oil, and the degree of deoxygenation was 53% at 500 °C.

However, catalyst deactivation of zeolite is a serious problem, which is known to be caused by pore blockage [9] because the HZSM-5 has only micropores (0.51–0.56 nm). Using a catalyst with a larger pore size could achieve an efficient reaction because the pore blockage would be suppressed. Adam et al [10] carried out pyrolysis of biomass using a mesoporous silica-alumina catalyst (Al-MCM-41), and an isomorphous catalyst with Si replaced by Cu (Cu-Al-MCM-41), which has a solid and mesoporous structure (d (100)= 3.7–4.5 nm). They reported that levoglucosan was not seen in the products using any catalyst. Acetic acid and furan yields increased, phenols with high molecular weight decreased, and using the catalyst increased yields of phenols and slightly increased those of hydrocarbons. An application of iron-loaded mesoporous silica-alumina catalyst to bio-oil was reported by Nilsen et al [11]. It is reported that this catalyst (Fe-Al-MCM-41) enhances dehydrogenation and increases coke and gas generation. Deoxygenation via the production of carbon oxides (CO, CO_2) is favored because the oxygen removal proceeds without hydrogen loss. Although, the effect of Al and Fe in catalytic cracking of bio-oil is not completely understood.

In this study, MCM-41 type mesoporous silica-alumina (MSAl) and iron loaded mesoporous silica (MS/Fe) were prepared, altering Al (1, 5 and 10 mol%) and Fe (1, 5 and 10 wt%) contents. In addition, iron loaded MSAl (MSAl/Fe) with different Al contents (1, 5 and 10 mol%) were also studied. The aim of this study is to clarify the effect of Al and Fe on the catalytic cracking of bio-oil using MCM-41-based catalysts.

EXPERIMENTAL

Bio-oil

Bio-oil, produced by the fast pyrolysis of Japanese cedar at 480 °C, was obtained from Azumasansho, Japan. The density, water content, ash content, and elemental composition of the bio-oil are shown in Table 1.

Table 1 Properties of the bio-oil

Density	1.2 g cm^{-3}
Water content	32.7 wt%
Ash content	1.0 wt%
Elemental composition	
C	51.6 wt%
H	6.6 wt%
O (diff.)	41.8 wt%

Catalyst preparation

Mesoporous silica-alumina (MSAl) catalysts were prepared by the sol-gel method. As a surfactant, 4.8 g of cetyltrimethyl ammonium bromide (CTAB, 13.2 mmol) was added to 240 mL of distilled water, together with 19.0 mL of 28% ammonia water. A mixture of tetraethyl orthosilicate and aluminum isopropoxide (Al content = 1, 5 and 10 mol%) was gradually added to the aqueous solution containing the surfactant. After stirring for 1 h, the precipitate was filtrated, washed with distilled water, and dried overnight at 60 °C. To remove the surfactant from the precipitate, it was heated to 300 °C for 0.5 h and kept at this temperature for 2 h followed by calcination at 600 °C for 5 h. This solid was crushed and sieved to a particle diameter of 250 μm. Hereafter, the products are designated as MSAl-1, MSAl-5 and MSAl-10.

An iron catalyst was loaded on the MSAl catalyst by a wet impregnation method. The MSAl (10 g) was immersed in 100 mL of distilled water containing $FeCl_2 \cdot 4H_2O$. The water was evaporated at 60 °C under vacuum conditions to deposit the iron precursor on the MSAl. The amount of iron was set at 10 wt% in this study. The products are designated as MSAl-1/Fe-10, MSAl-5/Fe-10 and MSAl-10/Fe-10. In addition, iron catalysts loaded on a commercial mesoporous silica (Tokyo Kasei, specific surface area: 276 $m^2 g^{-1}$, average pore diameter: 13.0 nm) were prepared by the same method as the MSAl/Fe catalysts. The MS catalysts containing 1, 5, and 10 wt% of iron are designated as MS/Fe-1, MS/Fe-5 and MS/Fe-10, respectively.

Characterization of the catalyst

Nitrogen adsorption was carried out at 77 K by BELSORP-mini II (Microtrac BEL). A pretreatment of the catalyst was carried out by heating at 150 °C for 5 h under vacuum conditions. Specific surface areas were calculated using the BET method in a relative pressure range between 0.05 and 0.25, while mode pore diameters were obtained by the BJH method. Powder X-ray diffraction (XRD) measurements of the catalysts were performed on an Ultima IV (Rigaku), using a Ni-filtered Cu Kα radiation (λ = 1.5406 Å) in order to confirm the crystal phase of the loaded iron. All XRD patterns of the catalysts before cracking (treated at 450 °C for 30 min in He 30 mL min^{-1}) were compared with those after cracking.

Catalytic cracking experiment

Catalytic cracking of the bio-oil was carried out using a fixed bed reactor (shown in Fig. 1) at ambient pressure. A catalyst (0.5 g) was put on quartz wool (0.2 g) in a Pyrex glass reactor without reduction. The reactor was purged by flowing He (150 mL min^{-1}) and heated at 450 °C. The bio-oil was introduced into the reactor by a syringe pump at a speed of 0.01 m min-1 together with He as a carrier gas (30 mL min^{-1}) for 300 min.

Liquid fractions produced during reaction were collected in a cold trap (-50 °C). Gaseous products such as CO, CO_2 and CH_4 were analyzed by an on-line gas chromatograph (Shimadzu GC2014) every 30 min. After the reaction, the color of the catalyst changed from white to gray or black. This is because the coke was deposited on the catalyst during the reaction. Accordingly, the coke yield (wt%) was calculated from the weight change in the catalyst before and after the reaction. The liquid fractions separated into two phases, water and reformed oil, and each yield (wt%) was calculated from the weight of each phase after separation. The increase in the weight of the cotton wool water trap was also included in the water yield.

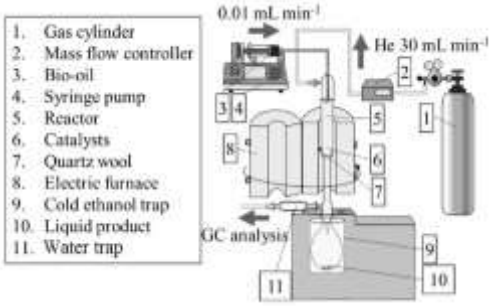

Fig. 1 Catalytic cracking apparatus

Characterization of the reformed oil

Identification and determination of constituents in the reformed oil were performed by a gas chromatograph mass spectrometer (Shimadzu GCMS-QP2010 SE). GC/MS analysis was carried out to confirm the change in the oil components before and after cracking. A sample (0.5 µl), which was made by diluting 1 µl of reformed oil with 1 mL of acetone, was analyzed using an Rtx-1 column (length: 30 m, film thickness: 0.25 µm, internal diameter: 0.25 mm). Substances were identified by collating their mass spectra with the database attached to the apparatus. IR spectra of the reformed oil were measured by FT-IR (Shimadzu, IR Affinity-1) using the ATR method. Measurement conditions were 16 scans and 2 cm^{-1} of resolution. A small amount of water was still present in the reformed oil phase. Thus, moisture content in the reformed oil was determined with a Karl Fischer titrator (KEM, MKA-610). The ultimate analysis was carried out using a HCN coder (YANACO, MT-700HCN). Oxygen content was calculated by subtracting hydrogen and carbon from the entire overall weight, since the raw material

of the bio-oil (Japanese cedar) contains little nitrogen or ash content. The elemental composition is shown on a wet basis since eliminating water is difficult.

RESULTS

Characterization of the catalysts

The specific surface areas and mode diameters of the catalysts are shown in Table 2. It was confirmed that all the catalysts had large surface areas and mode pore diameters.

Table 2 Results of N_2 adsorption

Sample	BET surface area / m^2 g^{-1}	Mode pore diameter / nm	Pore volume / cm^3
MSAl-1	1000	2.7	0.93
MSAl-5	1000	2.7	1.22
MSAl-10	900	2.7	1.08
MS/Fe-1	280	18.5	0.66
MS/Fe-5	240	18.5	0.68
MS/Fe-10	220	18.5	0.50
MSAl-1/Fe-10	700	2.7	1.28
MSAl-5/Fe-10	580	2.7	1.13
MSAl-10/Fe-10	510	2.7	0.98

The crystal phases of the loaded iron were identified by the XRD patterns (Figs. 2 (a)-(d)). Figs. 2 (a) and (b) show the XRD patterns of the catalysts before cracking (heating at 450 °C for 30 min in He atmosphere). Before cracking, only Fe_2O_3 (hematite) was observed, both in the MS/Fe and MSAl/Fe catalysts. However, the characteristic pattern of Fe_3O_4 (magnetite) appeared after cracking, while the peaks of hematite disappeared (Figs. 2(c), (d)). This suggests that the loaded iron changed into magnetite during the reaction.

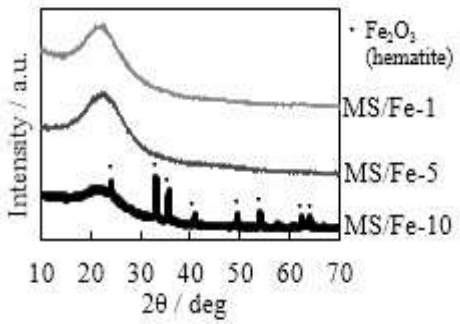

Fig. 2 (a) XRD patterns of MS/Fe before cracking

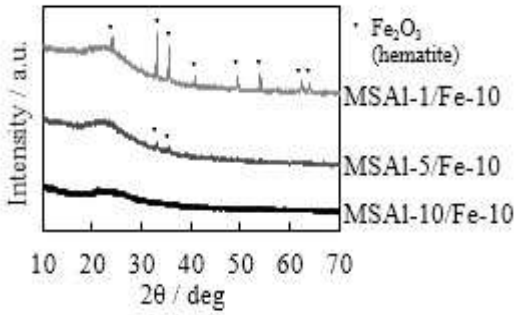

Fig. 2 (b) XRD patterns of MSAl/Fe before cracking

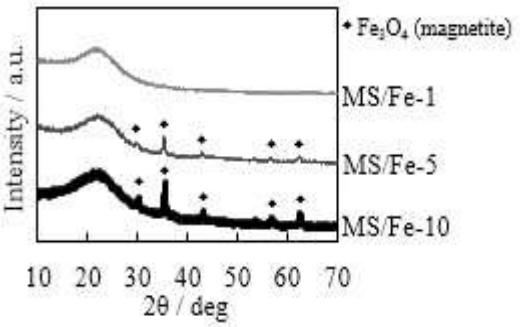

Fig. 2 (c) XRD patterns of MS/Fe after cracking

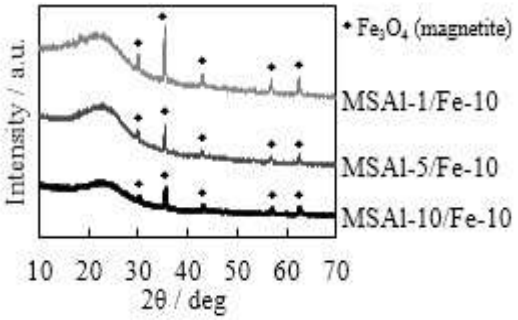

Fig. 2 (d) XRD patterns of MSAl/Fe after cracking

Product distribution

Product yields after catalytic cracking are shown in Table 3, together with the composition of the original bio-oil. Because the bio-oil before reaction contained 32.7 wt% of moisture, hereafter denoted as moisture, the resultant 67.3 wt% of the fraction was recognized as an organic component, denoted as organic.

In the case of catalytic cracking without a catalyst, the organic and moisture yields decreased to 49.3 and 5.7 wt%, respectively. Yields of CO and CO_2 were quite low at 0.1 wt% and 0.2 wt%, respectively, and the evolution of CH_4 was not detected. The coke formed (16.2 wt%) is derived from polymerization of organic [12] and non-volatile matter originally contained in the bio-oil. Accordingly, 65.5 wt% of the fraction, the sum of the organic yield and the coke yield, was regarded as the total organic yield. This value is almost the same as the organic yield before cracking. Therefore, the organic before cracking is partially converted into coke during the reformation. On the other hand, the unidentified component in Table 3 is mainly water which could not be completely collected in the cold trap. Accordingly, the sum of moisture, the water and the unidentified component was assumed to be the total water. (The reason why the unidentified component had the same composition as water is described in section "3.3 Elemental analysis".) Thus, the total water yield after cracking was almost the same as that before cracking. This result also suggests that the unidentified component is water.

When a catalyst other than MS/Fe-10 was used, the organic yield was commonly lower than it was without a catalyst. On the other hand, the coke yield increased when using any catalyst, indicating that the carbon was deposited on the catalyst surface.

In the MSAl catalysts, the total organic yields for MSAl-1, MSAl-5 and MSAl-10 were 62.6, 64.7 and 57.5 wt% ,

Table 3 Product yield before and after catalytic cracking

	Coke	Organic	Moisture	Water	CO	CO_2	CH_4	Unidentified	Total organic	Total water
Before cracking	-	67.3	32.7	-	-	-	-	-	67.3	32.7
No catalyst	16.2	49.3	5.7	11.1	0.1	0.2	0.0	17.4	65.5	34.2
MSAl-1	24.1	38.5	3.2	17.4	1.3	0.7	0.3	14.5	62.6	35.1
MSAl-5	19.7	45.0	4.1	15.9	0.9	0.4	0.2	13.9	64.7	33.9
MSAl-10	21.1	36.4	3.0	18.9	1.1	1.2	0.3	18	57.5	39.9
MS/Fe-1	19.0	46.8	3.9	12.6	1.4	1.5	0.3	14.5	65.8	31.0
MS/Fe-5	18.6	48.8	3.5	18.5	1.1	1.4	0.2	7.9	67.4	29.9
MS/Fe-10	19.1	51.2	3.4	15.4	1.7	2.3	0.5	6.4	70.3	25.2
MSAl-1 /Fe-10	23.8	43.8	2.9	11.8	2.1	2.1	0.5	13.0	67.6	27.7
MSAl-5 /Fe-10	20.4	44.8	3.0	18.5	2.9	2.9	0.7	6.8	65.2	28.3
MSAl-10 /Fe-10	25.4	43.3	3.1	13.8	2.4	3.1	0.5	8.4	68.3	25.7

respectively, which are lower than they were before cracking (67.3 wt%). In contrast, the yields of CO, CO_2 and CH_4 were slightly increased compared to those without catalysts. However, no clear relationship was seen between the yields and the Al content of the catalyst.

In the MS/Fe catalysts, the organic yield increased with increased Fe loading. The total organic yield also increased to 65.8, 67.4 and 70.3 wt% with increased Fe content, although the coke yields were almost the same.

By contrast, the total water yield decreased from 31.0 to 25.2 wt% when more iron was loaded on the catalyst. The yields of CO and CO_2 were higher than those in the MSAl catalysts.

In the MSAl/Fe catalysts, the total organic yield ranged from 65.2 to 68.3 wt% and was nearly equal to that before cracking. The highest yields of CO and CO_2 were obtained in MSAl/Fe catalysts while the total water yields (25.7–28.3 wt%) were as low as those of the MS/Fe catalysts.

Elemental analysis

Table 4 shows the elemental analyses of the oil phase before and after catalytic cracking. Each mass balance of C, H and O was calculated by multiplying the yield of each component and its elemental composition (Figs. 3 (a)-(c)).

Table 4 Ultimate analysis of bio-oil before and after cracking

	H / wt%	C / wt%	O (diff.) / wt%	H/C *)	O/C *)
Before cracking	6.6	51.6	41.8	1.52	0.61
No catalyst	6.5	61.8	31.6	1.25	0.38
MSAl-1	5.9	67.7	26.3	1.04	0.28
MSAl-5	5.7	69.4	24.9	0.98	0.27
MSAl-10	6.4	70.3	23.3	1.08	0.25
MS/Fe-1	6.3	68.6	25.1	1.04	0.24
MS/Fe-5	6.4	65.2	28.4	1.10	0.29
MS/Fe-10	6.6	63.5	29.9	1.20	0.32
MSAl-1/Fe-10	6.0	61.5	32.5	1.16	0.37
MSAl-5/Fe-10	6.6	66.3	27.2	1.19	0.28
MSAl-10/Fe-10	7.0	70.4	22.5	1.18	0.21

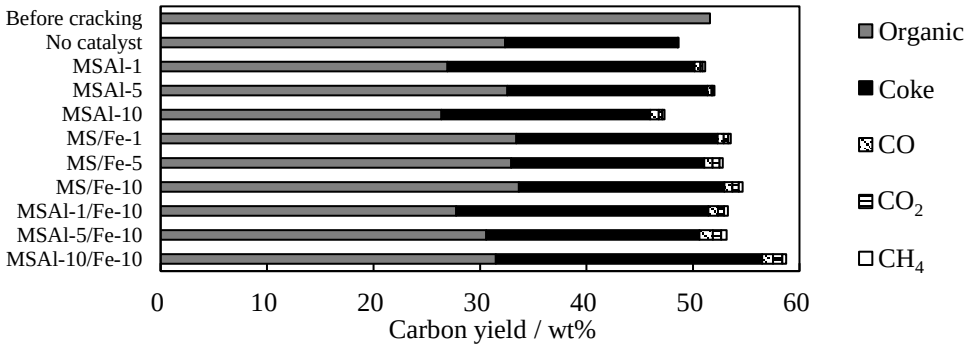

Fig. 3 (a) Carbon balance

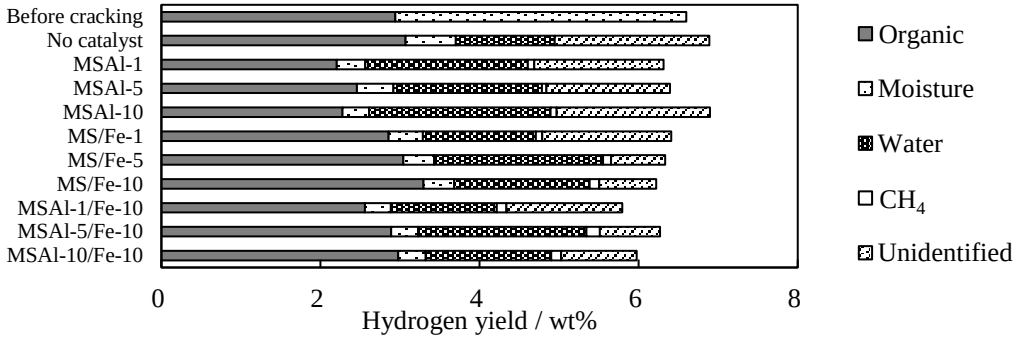

Fig. 3 (b) Hydrogen balance

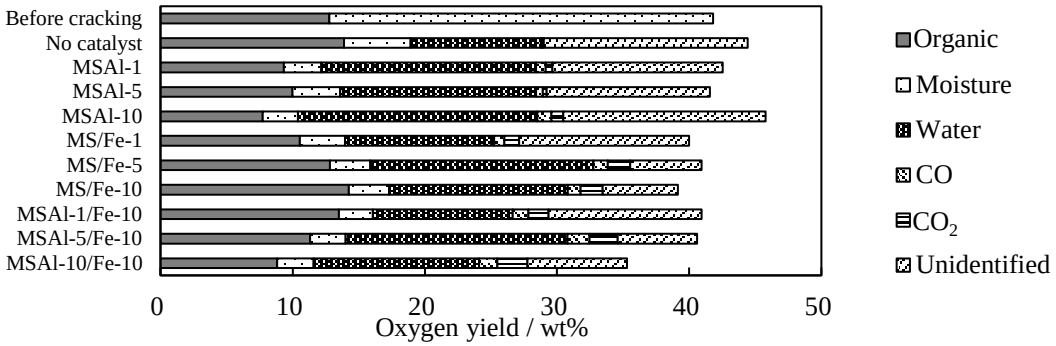

Fig. 3 (c) Oxygen balance

Most of the carbon in the original bio-oil was distributed to the coke and the organic when the coke was assumed to be pure carbon (Fig.3 (a)). Systematic change in the carbon distribution was not seen in the MSAl catalysts. In contrast, it was found that more carbon was distributed to the oil upon increasing the Al content in the MSAl/Fe catalysts. Such a change was not seen when the Fe content was increased in the MS/Fe catalysts.

Mass balances of hydrogen and oxygen were calculated assuming the unidentified component to be water. From Figs. 3 (b) and (c), it was found that the total amounts of hydrogen and oxygen were more than 84.4 mol%.

Mass balance of hydrogen and oxygen was almost achieved as well as the carbon balance. No relationship between the Al content in the MSAl catalyst and the hydrogen and oxygen in the oil was seen.

On the other hand, an increase in hydrogen and a decrease in oxygen distributed to the oil were observed upon increasing the Al content in the MSAl/Fe catalysts. It was found that both the hydrogen and oxygen in the oil increased when the amount of loaded Fe in the MS/Fe catalysts increased. A Van Krevelen diagram was made from the H/C an O/C molar ratios of the oil phase (Fig. 4). In this figure, the shift of the plot to the lower left side along the double line indicates dehydration, while the shift of the plot to the lower right side along the dotted line indicates demethylation. Likewise, the plot moves to the upper right side along the broken line when decarboxylation occurs. The H/C and O/C ratios of the bio-oil before cracking were 1.52 and 0.61, respectively. The dehydration of the oil took place after cracking, since all the plots are in the lower left side of the plot before cracking.

From this figure, it was found that more dehydration occurred in the MSAl-1 and MSAl-5 compared to the reaction without a catalyst, and the extent of dehydration in the MSAl-5 was larger than that in the MSAl-1. The plot of MSAl-10 is located to the upper left of the plot of MSAl-5, suggesting that decarboxylation and/or demethylation occurred as well as dehydration. In the MS/Fe catalysts, the plot shifted to the upper right side with increasing Fe content. Furthermore, the movement of the plot to the upper left side with increasing Al content was observed in the MSAl/Fe catalysts, indicating the progress of decarboxylation.

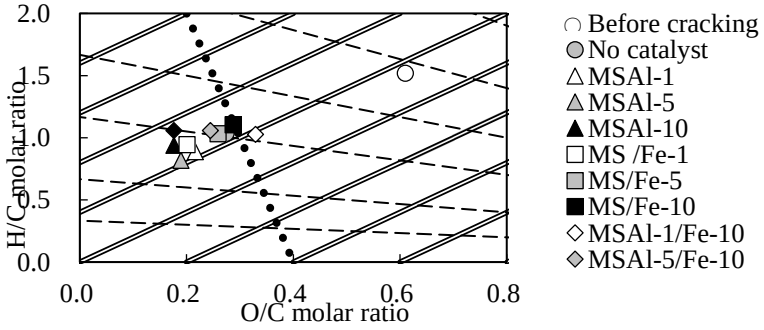

Fig. 4 Van Krevelen diagram

GC/MS analysis

The bio-oil before catalytic cracking was diluted with acetone as a solvent, as its viscosity was otherwise too high to allow injection into the GC/MS. Accordingly, all other oil samples were also diluted with acetone and analyzed for comparison. Some compounds, such as water and methanol, which possessed similar retention times to acetone, were not detected due to the excess acetone added to the reformed oil. As a result of analysis, no less than 70 % of compounds were identified, with more than 85% of similarity in all cases. Firstly, the relative areas of compounds classified by oxygen-containing functional groups were summed up for comparison, because the bio-oil is a mixture of highly variable substances. This classification makes possible the estimation of the relationship between the decomposition of oxygenated compounds and the progress of deoxygenation. Compounds with multiple oxygen-containing functional groups were classified according to instability and difficulty of deoxygenation, in the following order of priority: Phenols > Aldehydes > Ketones > Carboxylic acids > Esters > Ethers > Alcohols > Hydrocarbons. Table 5 shows the relative areas of the components. Half of the detected compounds was occupied by phenols in the bio-oil, both before and after catalytic cracking.

Table 5 GC/MS relative area of compounds contained in bio-oil before and after cracking

	Phenols	Aldehydes	Ketones	Acids	Esters	Ethers	Alcohols	Hydrocarbons	Unidentified
Before cracking	46.6	1.0	5.0	1.2	0.8	5.7	4.2	11.3	24.3
No catalyst	51.2	1.4	6.0	0.9	0.6	1.0	4.0	10.7	24.2
MSAl-1	52.6	1.7	5.3	0.9	0.6	3.5	0.0	15.0	20.6
MSAl-5	51.4	2.1	4.2	0.6	0.6	3.5	0.0	16.0	21.5
MSAl-10	49.9	1.6	4.1	0.5	0.4	3.6	0.0	16.0	23.8
MS/Fe-1	48.5	2.1	5.4	1.0	0.6	2.8	0.0	12.8	26.8
MS/Fe-5	52.6	1.2	5.5	0.8	1.0	3.0	1.7	9.6	24.7
MS/Fe-10	50.6	2.0	5.6	1.0	0.5	3.6	2.0	14.7	20.0
MSAl-1 /Fe-10	52.5	2.4	6.4	0.9	0.2	3.7	0.9	14.9	18.2
MSAl-5 /Fe-10	52.7	1.5	5.7	0.8	0.7	3.9	1.0	14.8	18.9
MSAl-10 /Fe-10	51.0	2.3	5.9	1.1	0.7	3.2	0.9	12.3	22.7

The catalytic cracking using the MSAl catalysts increased the relative area of hydrocarbons by 4.7–5.7% in comparison with the bio-oil before cracking. Moreover, whereas 4.2% of alcohols were included in the original bio-oil, none were detected after the catalytic cracking. The phenols had a decreasing tendency with increasing Al content in the MSAl catalysts (MSAl-1 > MSAl-5 > MSAl-10). In the MS/Fe catalysts, a tendency for alcohols to increase with increasing iron loadings was observed. Alcohols were also detected in the oil after catalytic cracking using the MSAl/Fe catalysts. However, a systematic change in the components with an increase in the Al content was not evident. There was almost no difference between the MSAl-1/Fe-10 and the MSAl-5/Fe-10 across all components. In contrast, the relative area for MSAl-10/Fe-10 showed decreases in the phenols and hydrocarbons, by 1.5–1.7% and 2.5–2.6% respectively (4.1–4.2% in total), and an increase in the unidentified component by 3.8–4.5%.

As described above, phenols occupied half of the bio-oil component. Accordingly, the phenols were further classified into three types by the number of oxygen-containing functional groups; i.e., monosubstituted, disubstituted and trisubstituted phenols, which were designated as P1, P2, and P3, respectively. A decrease in the number of oxygen-containing functional groups suggests the progress of deoxygenation, even if the phenols were not decomposed completely.

Figs. 5 (a)-(c) shows the changes in P1, P2 and P3 for the MSAl, MS/Fe and MSAl/Fe catalysts. The horizontal axis in these figures is the Al content or the amount of loaded Fe. The relative ratios in the reformed bio-oil without

catalyst were used as the data for Al 0 mol% and Fe 0 wt%. When the Al content in the MSAl catalysts increased from 0 mol% to 5 mol%, the P1 increased by 6.6%, and the P2 decreased by 5.5%. However, further increase in the Al content did not change the relative areas of either P1 or P2. There was only a small quantity of P3 throughout the change in the Al content.

In the MS/Fe catalysts, P1 increased by 11.7% and P2 decreased by 11.2% when the amount of loaded iron increased from 0 wt% to 5 wt%. In contrast, changes in both P1 and P2 were smaller when 10 wt% of Fe was loaded. Only a small amount of P3 was detected, as well as the MSAl catalysts. The MSAl/Fe catalysts increased 11.0% of the P1 and decreased 11.0% of the P2 when the Al content increased from 0 mol% to 1 mol%. However, only a slight change was seen in P1 and P2, even though more Al was added to the catalysts. P3 did not show any major change either.

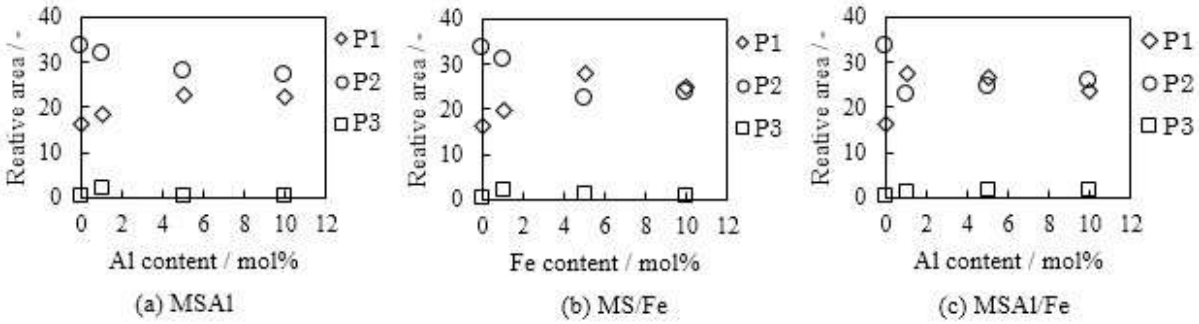

Figs. 5 (a)-(c) Relationship between Al or Fe content and phenols

FT-IR

IR spectra of the bio-oil before and after cracking are shown in Fig. 6, and peak assignment is shown in Table 6. Comparing the spectra before and after cracking, profile changes appeared in the region of 3000–3700 cm^{-1} and 1600–1710 cm^{-1}, which are assigned mainly to OH stretching and C=C or C=O stretching, respectively. The band of OH stretching decreased when the bio-oil was reformed without a catalyst.

In the MSAl catalysts, the absorption of OH stretching decreased compared to that before cracking, and the lowest absorption was shown in the MSAl-5. The band at 1600–1710 cm^{-1} split into two peaks in the MSAl-10. In the MS/Fe catalysts, the band at 3000–3700 cm^{-1} decreased upon increasing the amount of loaded Fe. Split peaks in the 1600–1710 cm^{-1} band were also seen in these catalysts.

In the MSAl/Fe catalysts, the band assigned to the OH stretching decreased when more Al was introduced to the catalysts. As is the case with the MS/Fe catalysts, the band at 1600–1710 cm^{-1} was divided into two peaks.

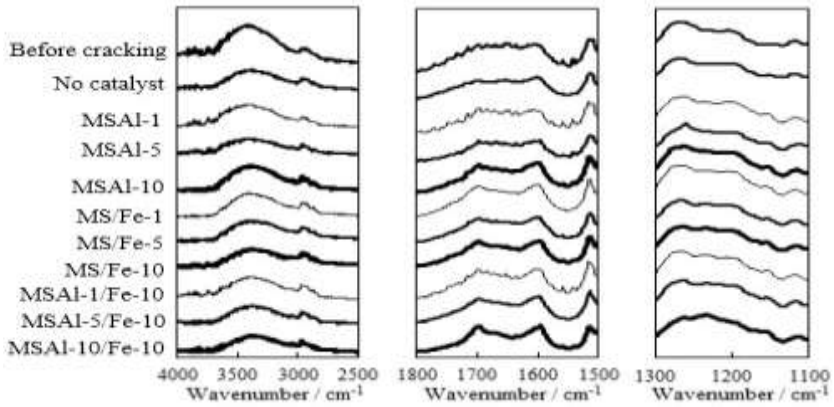

Fig. 6 IR spectra of bio-oil before and after catalytic cracking

Table 6 Peak assignments of IR spectra [13-24]

Wavenumber / cm^{-1}	Assignment
3000 – 3700	O-H stretching
2800 – 3000	aliphatic C-H stretching
1654 – 1710	antisymmetric vibrations of conjugated diketones [13], absorption of unsaturated ketones, unsaturated aldehydes and aryl aldehydes, hydroxy unsaturated ketones and hydroxy aldehydes [14]
1646	water (H-O-H) absorption [15]
1643	symmetric vibrations of the conjugated ketones [13]
1600 – 1640	C=C stretching [16]
1514	aromatic skeletal vibrations [17]
1452, 1454	C-H stretching bends and deformations in the methyl groups and the methylene groups [18]
1372	C-H bending [17]
1200 – 1300	ethereal (C-O-C) and alcoholic (C-OH) units [19], phenol (-OH bending) [18], C-O stretch in ester and ether [20], C-O stretching (R-COOH), C-C skeleton (R-CO-R') [21]
1155	C-O stretch in esters [22]
1111	C-OH skeletal vibration [17]
1088	C-O stretching [18]
1030 – 1050	C-O stretching [18], C-O-C pyranose ring skeletal vibration [17]
816	C-H out of plane bending vibration from aromatics and their derivatives [18]
748	C-H out of plane bending vibration from aromatics and their derivatives [18]

DISCUSSION

The effect of thermal cracking (No catalyst)

The reforming of bio-oil without a catalyst is considered to cause only thermal cracking of the bio-oil. The water content of the oil after reforming was 10.3 wt%, and decreased to less than 1/3 of its value before cracking (32.7 wt%). On the other hand, the total organic and total water yields after reforming without a catalyst were almost the same as those in the original bio-oil. These results suggest that water was only separated from the oil by reforming without a catalyst, resulting in a decrease in the absorbance of the OH stretching in the FT-IR spectrum. Meanwhile, the deposition of a considerable amount of coke was observed. It is reported that the C-O stretching attributed to the guaiacyl and syringyl unit [23], which are constituents of lignin, appeared at 1260–1270 cm^{-1} in the FT-IR spectrum; and the bio-oil contains lignin oligomers of which molecular mass distributes up to 1500 [24]. Because the adsorption at 1260–1270 cm^{-1} was decreased when the bio-oil was reformed without a catalyst, it is considered that most of the part produced by thermal cracking of the bio-oil was deposited as coke on the quartz wool, and a simultaneous decrease in ethers and increase in phenols took place (Table 5).

The effect of Al content (MSAl catalysts)

The lower total organic yields when the MSAl catalysts were used (57.5–64.7 wt%), compared to that before cracking (67.3 wt%), indicate decomposition of the organic component. The gas (CO, CO_2 and CH_4) yields were higher than those without a catalyst. In addition, the progress of dehydration is inferred from the increase in the total water yields and the shift of the plot to the lower left side in the Van Krevelen diagram. The decrease in the OH stretching absorption, the absence of detectable alcohols (4.2 wt% in the original bio-oil), and the decrease in P2 phenols, also suggest that the dehydration reaction occurred because of the MSAl catalysts. In contrast, the hydrocarbons increased by 4.7–5.7 wt%, suggesting that the dehydration of the alcohols and phenols was promoted by the acid sites on the MSAl catalysts. However, no significant difference between the water content of the oil obtained from reforming without a catalyst (10.3 wt%) and with the MSAl catalysts (7.6–8.3 wt%) was observed (Table 7). Therefore, it is suggested that decomposition of the hydroxyl group occurred along with water separation from the original bio-oil.

Next, the effect of the Al content on the product distribution is considered. There was no systematic change in the organic and coke yields with the change in the Al content. This indicates that the catalysis differs among the MSAl catalysts with different amounts of Al. The absorbance of the OH stretching vibration decreased upon increasing the Al content up to 5 mol%, indicating that MSAl catalysts with Al content up to 5 mol% promote the decomposition of the hydroxyl group. When the Al content in the MSAl catalyst was increased to 10 mol%, the band around 1654–1710 cm^{-1} (attributed to the conjugated ketones, hydroxyl unsaturated ketones, and hydroxyl unsaturated aldehydes) decreased. This result indicates that a different reaction also occurred, accompanied by the generation of the hydroxyl group, unlike catalysts with Al content up to 5 mol%.

The effect of Fe content (MS/Fe catalysts)

The organic and total organic yields increased upon increasing the amount of loaded Fe, while the total water yields decreased. In addition, the yields of CO and CO_2 increased with increased iron loadings. It should be noted that both the hydrogen and oxygen contents in the oil phase increased (Table 4). The alcohols and P1 phenols in the reformed oil also increased when more iron was loaded (Table 5 and Fig. 5). Also, the vibration of OH stretching in the FT-IR weakened, and the oil (moisture) yields decreased. The absorption of C=O stretching (1654–1710 cm^{-1}) attributed to the conjugated ketones decreased. These changes were probably caused by the reaction between the organics and water on the iron catalyst. From the results of XRD (Figs. 2), it became clear that the catalyst was reduced from Fe_2O_3 (hematite) to Fe_3O_4 (magnetite). Magnetite, which is a complex oxide composed of Fe(II) and Fe(III), is known to be stable in water vapor [25]. Considering that the bio-oil used in this experiment contained 32.7 wt% of water, it is suggested that the magnetite present in a stable state promoted the decarboxylation reaction. Accordingly, it is estimated that the MS/Fe catalysts promote the decarboxylation reaction between the organics and water. Simultaneously, the organics are oxidized, producing the oxygen-containing compounds such as alcohols and ethers. It should be concluded that the addition of iron is not suitable for the deoxygenation, because the oxygen content in the reformed bio-oil using the MS/Fe catalysts was larger than that using the MSAl catalysts.

The effect of the MSAl/Fe catalyst

The total organic yields (65.2–68.3 wt%) were almost the same as those in the original bio-oil, while the total water (25.7–28.3 wt%) yields decreased. Moreover, CO and CO_2 yields were the highest among all the catalysts used in this study. These results indicate that the MSAl/Fe catalysts promote the decarboxylation reaction between organics and water, like the MS/Fe catalysts.

Interestingly, the plot in the Van Krevelen diagram shifted to the upper left with increasing Al content in the MSAl/Fe catalysts, indicating that the decarboxylation reaction proceeded. This promotion of the decarboxylation reaction is also suggested from the lowest absorption of conjugated ketones (1654–1710 cm^{-1}) among the catalysts used in this study. The MSAl/Fe catalysts showed a decrease in alcohols (Table 5) and an increase in ethers and esters (Table 5 and Fig. 6) compared to the results obtained from the MS/Fe-10 catalyst. Thus, the MSAl/Fe catalysts are considered to promote dehydration via the decomposition of the hydroxyl group.

Thus, the oxygen content in the MSAl/Fe catalysts were the lowest among the tested catalysts (Table 4), resulting in relatively high heating values (Table 7). It was proved that the MSAl-10/Fe-10, which is considered to promote both decarboxylation and dehydration, is the most effective deoxygenation catalyst among the catalysts used in this study.

CONCLUSION

Catalysts based on MCM-41 type mesoporous silica were prepared and used in the catalytic cracking of bio-oil at 450 °C, under ambient pressure in a He atmosphere. When the mesoporous silica-alumina (MSAl) catalysts with different Al content were used, the dehydration reaction was promoted by increasing the Al content. When iron-loaded mesoporous silica (MS/Fe) catalysts were used, the hydrolysis reaction was promoted by increasing the Fe loading. Using MSAl/Fe catalysts, which were prepared by the impregnation of iron chloride on the MSAl catalysts, the decarboxylation reaction was promoted by increasing the Al content of the catalyst. From the GC/MS measurements, all the bio-oils before and after catalytic cracking were proven to be rich in phenols. For the MSAl/Fe catalysts, the differences between the IR spectra before and after catalytic cracking suggest decomposition of the conjugated ketones, which is possibly related to the reforming of the bio-oil.

ACKNOWLEDGEMENTS
We would like to thank Editage (www.editage.jp) for English language editing.

REFERENCES
1. Fengel D, Wegner G. "Wood: Chemistry Ultrastructure, Reactions" Walter de Gruyter: Berlin and New York, 1984; pp 167-175.
2. Lawoko M, Henriksson G, Gellerstedt G. "Characterisation of lignin-carbohydrate complexes (LCCs) of spruce wood (Picea abies L.)" Holzforschung 2006; **66 (2)**: 156-161.
3. Qi Z, Jie C, Tiejun W, Ying X. "Review of biomass pyrolysis oil properties and upgrading research" Energy Conversion and Management, 2007; **48**: 87-92.
4. Guo Y, Wang Y, Wei F, Jin Y. "Research progress in biomass flash pyrolysis technology for liquids production" Chemical Industry Engineering Progress 2001; **8**: 13-17.
5. Oasmaa A, Czernik S, "Fuel oil quality of biomass pyrolysis oils-state of the art for the end -users" Energy Fuels 1999; **13**: 914-921.
6. Mortensen PM, Grunwaldt JD, Jensen PA, Knudsen KG, Jensen AD. "A review of catalytic upgrading of bio-oil to engine fuels" Applied Catalysis A: General, 2011; **407**: 87-92.
7. Radlein D, Quignard A. "A short historical review of fast pyrolysis of biomass" Oil & Gas Science and Technology – Rev. IFP Energies nouvelles, 2013; **68 (4)**: 765-783.
8. Williams PT, Horne PA. "Characterisation of oils from the fluidised bed pyrolysis of biomass with zeolite catalyst upgrading" Biomass and Bioenergy, 1994; **7**, 223-236.
9. Froment GF. "A quantitative approach of catalyst deactivation by coke formation" Catalyst Deactivation, 1980; **6**: 1-19.
10. Adam J, Blazsó M, Mészáros E, Stöcker M, Nilsen MH, Bouzga A, Hustad JE, Grønli M, Øye G. "Pyrolysis of biomass in the presence of Al-MCM-41 type catalysts" Fuel, 2005; **84**: 1494-1502.
11. Nilsen MH, Antonakou E, Bouzga, A, Lappas A, Mathisen K, Stöcker M. "Investigation of the effect of metal sites in Me-Al-MCM-41 (Me = Fe, Cu or Zn) on the catalytic behavior during the pyrolysis of wooden based biomass" Microporous and Mesoporous Materials, 2007; **105**: 189-203.
12. Gholizadeh M, Gunawan R, Hu X, Mercader FM, Westerhof R, Chaitwat W, Hasan MM, Mourant D, Li CZ. "Effects of temperature on the hydrotreatment behavior of pyrolysis bio-oil and coke formation in a continuous hydrotreatment reactor" Fuel Processing Technology, 2016; **148**: 175-183.
13. Łojewski T, Miśkowiec P, Missori M, Lubańska A, Proniewicz LM, Łojewska J. "FTIR and UV/vis as methods for evaluation of oxidative degradation of model paper: DFT approach for carbonyl vibrations." Carbohydrate Polymers, 2010; **82**: 370-375.
14. Lievens C, Mourant D, He M, Gunawan R, Li X, Li CZ. "An FT-IR spectroscopic study of carbonyl functionalities in bio-oils" Fuel, 2011; **90**: 3417–3423.
15. Dang TP, Le GH, Pham TTG, Nguyen TK, Dao DC, Vu TMH, Hoang TTT, Tran TKH, Vu AT. "Synthesis of advanced materials for bio-oil production from rice straw by pyrolysis" Advances in Natural Sciences: Nanoscience and Nanotechnology, 2011; **2 (4)**: 1-6.
16. Krishna BB, Biswas B, Ohri P, Kumar J, Singh R, Bhaskar T. "Pyrolysis of Cedrus deodara saw mill shavings in hydrogen and nitrogen atmosphere for the production of bio-oil" Renewable Energy, 2016; **98**: 238-244.
17. Ma HH, Zhang BX, Zhang P, Li S, Gao YF, Hu XM. "An efficient process for lignin extraction and enzymatic hydrolysis of corn stalk by pyrrolidonium ionic liquids" Fuel Processing Technology, 2016; **148**: 138-145.
18. Yang T, Jie Y, Li B, Kai X, Yan Z, Li R. "Catalytic hydrodeoxygenation of crude bio-oil over an unsupported bimetallic dispersed catalyst in supercritical ethanol" Fuel Processing Technology, 2016; **148**: 19-27.
19. Xu J, Jiang J, Dai W, Xu Y. "Liquefaction of sawdust in hot compressed ethanol for the production of bio-oils" Process Safety and Environmental Protection, 2012; **90**: 333-338.
20. Zhang X, Chen L, Kong W, Wang T, Zhang Q, Long J, Xu Y, Ma L. "Upgrading of bio-oil to boiler fuel by catalytic hydrotreatment and esterification in an efficient process" Energy, 2015; **84**: 83-90.
21. Shen DK, Gu S, Bridgwater AV. "Study on the pyrolytic behaviour of xylan-based hemicellulose using TG-FTIR and Py-GC-FTIR" Journal of Analytical and Applied Pyrolysis, 2010; **87**: 199-206.

22. Hilten RN, Das KC. "Comparison of three accelerated aging procedures to assess bio-oil stability" Fuel, 2010; **89**: 2741-2749.
23. Liu Q, Wang S, Zheng Y, Luo Z, Cen K. "Mechanism study of wood lignin pyrolysis by using TG–FTIR analysis" Journal of Analytical and Applied Pyrolysis, 2008; **82**: 170-177.
24. Meesuk S, Cao JP, Sato K, Ogawa Y, Takarada T. "The effects of temperature on product yields and composition of bio-oils in hydropyrolysis of rice husk using nickel-loaded brown coal char catalyst" Journal of Analytical and Applied Pyrolysis, 2012; **94**: 238-245.
25. Svoboda K, Slowinski G, Rogut J, Baxter D. "Thermodynamic possibilities and constraints for pure hydrogen production by iron based chemical looping process at lower temperatures" Energy Conversion and Management, 2007; **48**: 3063-3073.